Spectroscopic Signature of Non-Maxwellian and Nonstationary Effects in Plasmas Heated by Intense, Ultrashort Laser Pulses

J. P. Matte, J. C. Kieffer, S. Ethier, and M. Chaker
Institut National de la Recherche Scientifique, Energie et Matériaux, 1650 Montée Ste-Julie, C.P. 1020, Varennes, Québec, Canada J3X-1S2

O. Peyrusse
Commissariat à l'Energie Atomique, Limeil-Valenton, 94195 Villeneuve-St-Georges Cedex, France
(Received 24 September 1993)

The interaction of an intense (10^{16} W/cm^2), ultrashort (400 fs) 1.06 μm laser pulse normally incident on an aluminum preformed plasma was simulated with an electron kinetic code. Postprocessing with a detailed atomic model predicted the resulting K-shell x-ray spectrum. Both the very rapid time variation and the non-Maxwellian energy distribution (due to the steep gradients, energetic electrons stream from the hot into the cold plasma and enhance the excitation of Li-like satellites there) greatly modify the line ratios, even without any addition of hot electrons.

PACS numbers: 52.50.Jm, 44.10.+i, 52.25.Nr, 52.65.+z

Plasmas produced and heated by ultrashort (subpicosecond) laser pulses are at present being studied very actively, both for their novel fundamental properties and their potential applications. Among these, one of the most interesting is the production of intense, ultrashort x-ray pulses, which could in turn be used for x-ray microscopy or to photopump an x-ray laser, in contexts where subpicosecond time resolution is desired. These possibilities are due to the unique properties of these plasmas: extremely high energy density and highly transient, nonequilibrium states of matter, resulting from the exceedingly short temporal and spatial scales involved [1–8].

X-ray spectroscopy [9,10], and particularly ratios of Li-like satellite lines ($1s2l2l'$-$1s^22l$) [6,10], is a very important plasma diagnostic, and how these unique properties affect the spectra is the subject of the present work. The traditional analysis of these ratios, assuming Maxwellian electron energy distributions and steady state, is applicable for both an ultrashort pulse incident on a solid density plasma (the line ratios then have Boltzmann equilibrium values [6]), and for the case of a sufficiently long pulse, where the x-ray spectrum is characteristic of the considerably lower density at which the emission occurs. In this Letter, we present the first time dependent calculations of x-ray spectra emitted by preformed plasmas driven into a strongly non-Maxwellian state by an intense, ultrashort laser pulse.

Previous electron kinetic simulations of fully stripped plasmas have shown that, in steep electron temperature gradients (here, temperature means $\frac{2}{3}$ the average energy), energetic electrons stream into the cold plasma before they can be thermalized, and therefore, there is a surplus of these, compared to a Maxwellian at the local temperature [11–13], even in plasmas heated by nanosecond laser pulses [14,15]. An important consequence of this streaming effect is the preheating of the cold zones, and it can be included in fluid codes by using one of the various "delocalization models" [16–18] to calculate electron heat flow. However, in such fluid modeling, Maxwellian electron energy distributions are assumed for computing the rates of ionization and excitation.

Recently, x-ray line polarization measurements demonstrated anisotropy in the hot, underdense plasma, in approximate agreement with kinetic simulations [19]. It has also been shown that a minority hot Maxwellian component added to a thermal Maxwellian distribution enhances the rates [20], but no systematic, kinetic study of the atomic physics consequences of the deformation of the electron energy distribution in the colder parts of laser-heated plasmas has yet been published.

The present Letter focuses on the consequences of both the non-Maxwellian electron energy distributions and of the rapid time variation on the atomic physics (ionization, excitation, etc.). Specifically, we look at K-shell emission of Al ions, near 1.6 keV, because the atomic structure data of aluminum are quite well known, and this material is very convenient for experiments. We have performed a series of simulations of intense (10^{16} W/cm^2), ultrashort (400 fs FWHM, Gaussian) 1.06 μm laser pulses normally incident on an Al preformed plasma.

The plasma behavior was modeled with our electron kinetic code FPI [12,15] which includes the following: Coulomb collisions, transport, an electric field for quasineutrality, cold fluid ions hydrodynamics, and collisional absorption of the laser energy (with a kinetic heating operator [21]). Contrary to the analyses performed for recent short pulse experiments, at higher intensity [7] or oblique incidence [8], no hot electron source such as resonance absorption was added. Although it can never be totally excluded in practice, we chose to omit it because, in the experiments to which we will refer below, it was minimized by using a tightly focused normally incident

0031-9007/94/72(8)/1208(4)$06.00

beam, and also because the purpose of the present study is to focus on how the streaming effect modifies the emission spectrum. Additions were made to adapt the code to short pulse modeling: a wave solver [3], to better model absorption when the density gradient length is shorter than the laser wavelength, and a simplified average ion model, to take into account the cooling of electrons by ionization and excitation. We do not simulate the prepulse, but rather vary the initial (exponential) density scale length over a very wide range: from 10 μm to as low as 0.0035 μm (for 0.53 μm wavelength) to assess its effect. The simulations were started a few picoseconds before the peak of the laser pulse, and stopped 3–20 psec after, depending on the density gradient length.

During each kinetic simulation, at regular intervals, the entire energy distribution function [i.e., the isotropic component $f_0(x,v,t)$ of the electron velocity distribution function] as well as the ion density and hydrodynamic velocity profiles were recorded, and subsequently used as input for the multicell collisional-radiative atomic physics code TRANSPEC [22]. It includes all the ionization states, with a detailed description of H, He, and Li-like ionization stages and their excited states (as satellite line emission occurs mainly during the ionization phase, recombination from Li-like into Be-like levels need not be described in detail). Radiative transfer on optically thick lines (including the effect of the Doppler shift caused by hydrodynamic motion) is coupled self-consistently with the population kinetics calculation. We use simple Voigt line profiles because Stark broadening is small in preformed plasmas [23]. Only nine lines have a nonnegligible optical depth: the three He-like resonance lines, He-α,β,γ and six Li-like satellite lines: $1s2l2l' \rightarrow 1s^2 2l$. After the populations have been computed in each cell, for a given time, we predict the emerging spectrum as it would be observed at a 45° angle with respect to the laser axis. In Fig. 1, we illustrate a final result of this whole procedure with a time-dependent x-ray spectrum in the range of the He-α line and its Li-like $1s2l2l'$-$1s^2 2l$ satellites. Time integration of such a spectrum gives a time integrated synthetic spectrum, from which line ratios can be obtained. TRANSPEC was used in three modes to see which effects dominate. In the non-Maxwellian time-dependent (NMTD) mode (used in Fig. 1), the rates of ionization, excitation, and recombination (radiative and dielectronic) are obtained by performing the appropriate integral over the energy distribution function:

$$\text{Rate} = N_e\langle\sigma v\rangle = \int \sigma(v) f(\mathbf{v}) v d^3 v$$

$$= 4\pi \int \sigma(v) f_0(x,v,t) v^3 dv ,$$

where $\sigma(v)$ is the velocity dependent cross section for the transition, and $v = |\mathbf{v}|$. This is done for each spatial cell, at each time step of the atomic physics calculation, and for every rate, except for three-body recombination, because energetic electrons are unimportant for it, and the Maxwellian rate is adequate. In the Maxwellian time-dependent (MTD) mode, all rates are computed assuming a Maxwellian of the same density and temperature. In the Maxwellian steady state (MSS) mode, these same rates are used, and a steady state is assumed.

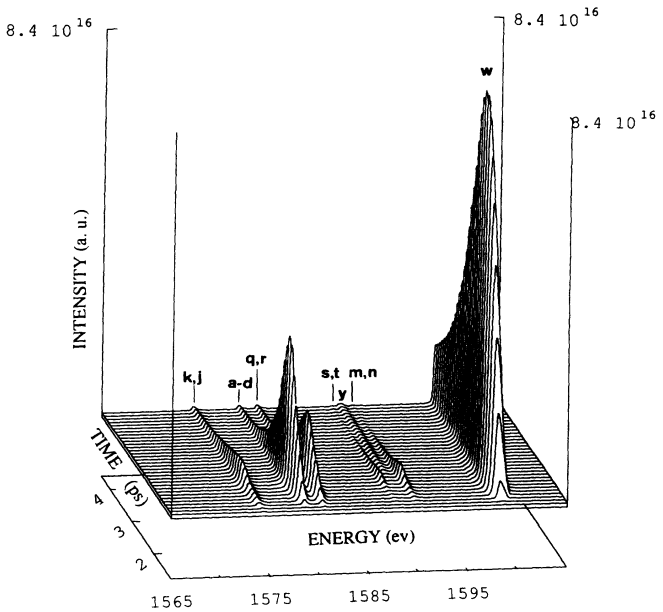

FIG. 1. Synthetic, time-dependent spectrum near the He-α line for the simulation with initial density scale length 1 μm (intensity, 10^6 W/cm^2; 400 fs FWHM; wavelength, 1.06 μm). Lines are labeled following the Gabriel notation [10].

Non-Maxwellian modification of the rates is most dramatic for density gradient lengths shorter than 0.1 μm: Absorption then occurs at very high density; the maximum temperature is only 400 eV, so that the 1.6 keV electrons are nonthermal and gradients are extremely steep. However, the density at which emission occurs is then so high [24] that collisional mixing imposes Boltzmann equilibrium among all the upper levels of the Li-like satellite lines, and this has been observed experimentally with 0.53 μm irradiation [23,25]. Thus, nonequilibrium effects cannot be diagnosed from these line ratios in such cases.

When the gradient length is 0.4 μm or more, absorption occurs near critical density (10^{21} cm^{-3}), at a 1–2 keV temperature. Then, the density at which emission occurs is not so high, and collisional mixing is less pronounced. Non-Maxwellian behavior, again for the 1 μm gradient length simulation, at the peak of the pulse, is illustrated in Figs. 2 and 3. In Fig. 2, we show the electron energy distribution itself at three positions in space and also the Maxwellians of equal density and temperature. The arrow at 1.6 keV shows the threshold for K-shell excitation. In Fig. 3, we have plotted, aside from the electron density and temperature profiles, the products

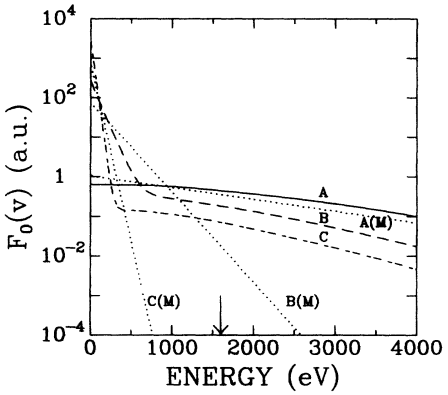

FIG. 2. Electron energy distributions (up to 4 keV) at three positions, at the peak of the pulse, for the same simulation as in Fig. 1. The arrow indicates the threshold for K-shell excitation. Densities and temperatures: 0.95, 3.5, 6.5×10^{21} cm^{-3}; and 1470, 191, and 49 eV for curves A, B, and C, respectively. The dotted lines are Maxwellians at the same density and temperature.

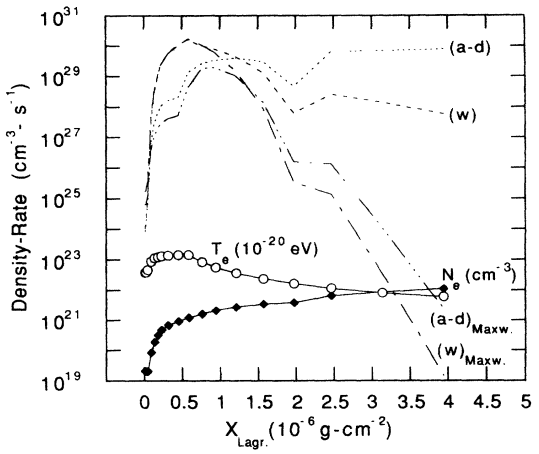

FIG. 3. Profiles of electron density (N_e) and temperature (T_e); density-rate products $N_{He}N_e\langle\sigma v\rangle$ of the He-α resonance line with non-Maxwellian W and W_{maxw} energy distributions; and $N_{Li}N_e\langle\sigma v\rangle$ of the Li-like (a-d) satellite lines with non-Maxwellian (a-d) and Maxwellian (a-d)$_{maxw}$ energy distributions, at the peak of the pulse, for the same simulation as in Fig. 1. The laser beam is incident from the left.

$N_{He}N_e\langle\sigma_w v\rangle$ and $N_{Li}N_e\langle\sigma_{a\text{-}d} v\rangle$ of He-like and Li-like ground state ion density times the excitation rate of the He-α resonance line (w line) and the collisional core excited (a-d) satellites, respectively, and the Maxwellian density-rate products, for comparison. It is at densities near critical, where absorption takes place and the temperature is highest, that much of the He-α emission originates. There, the deformation of the energy distribution by collisional heating [14,15,21] is very clearly seen (Fig. 2, curve A), but the reduction of the rates is modest because the local temperature is comparable to the threshold. On the contrary, in the somewhat denser and cooler regions, which are richer in Li-like ions, the density of 1.6 keV electrons is far above what would be expected for a Maxwellian at the local temperature, due to the streaming effect evoked above (Fig. 2, curve B), and the rate of excitation of Li-like collisional (a-d) satellite lines is therefore greatly enhanced. In the very dense and cold plasma, the degree of ionization is low and it is cold K-α emission which could be enhanced by the tail of the distribution (Fig. 2, curve C).

In Table I, we list the time integrated line ratios predicted for our simulations with four assumed initial density scale lengths: 0.4, 1, 4, and 10 μm, and the different TRANSPEC modes. Both the w (He-α) line and the dielectronic recombination satellites (k,j) are relatively insensitive to the non-Maxwellian effects, because He-like ions are dominant in the hotter regions, where the temperature is comparable to the excitation threshold. However, the $w/(k,j)$ line ratio is very sensitive to the density scale length: At short scale length, the density is moderately high and the levels responsible for (k,j) emission are quenched by collisional mixing with other doubly excited states; and also, the w line is very sensitive to reabsorption at longer scale lengths. On the other hand, the

TABLE I. Predicted time integrated line ratios, for different initial density scale lengths, and different TRANSPEC modes (M: Maxwellian; NM: non-Maxwellian; SS: steady state; TD: time-dependent); and measured values at 1.06 μm laser wavelength [24] (EXP). The underscored values come from time integrating the spectrum shown in Fig. 1; the others from analogous spectra.

	Scale length (μm)				
Line ratio (model)	0.4	1.0	4.0	10.0	EXP. [24]
W/kj (NMTD)	17.0	<u>16.8</u>	5.7	4.6	15 ± 1
ad/W (NMTD)	0.15	<u>0.23</u>	0.25	0.19	0.24 ± 0.02
ad/W (MTD)	0.12	0.08	0.17	0.16	
ad/W (MSS)	0.05	0.05	0.10	0.10	
ad/kj (NMTD)	2.56	<u>3.9</u>	1.4	0.86	3.0 ± 0.5
ad/kj (MTD)	1.75	1.4	1.0	0.78	
ad/kj (MSS)	0.82	0.78	0.77	0.83	

collisional core excited $(a\text{-}d)$ lines are very sensitive to the non-Maxwellian effects, as noted above. The $(a\text{-}d)/w$ line ratio indicates clearly that both time-dependent *and* non-Maxwellian effects need to be taken into account, but it is not very sensitive to the scale length. The $(a\text{-}d)/(k,j)$ line ratio is seen to depend strongly on the scale length, *and* also on the non-Maxwellian, and time-dependent effects. The enhancement of the $(a\text{-}d)$ Li-like satellites exists in the longer gradient length simulations, but it is less important because the streaming effect is then less pronounced, and $(a\text{-}d)$ satellite emission comes from warm regions where the overabundance of Li-like ions is due essentially to the fact that the ionization balance lags behind the equilibrium state. For all of the gradient lengths, comparing the Maxwellian steady state and time-dependent calculations shows the crucial importance of transient effects: The very rapid heating means that emission occurs before the ionization balance can come to equilibrium, hence the enhancement of the $(a\text{-}d)$ Li-like satellite lines. However, the supplementary enhancement due to the streaming effect (NMTD, 1 μm) is clearly essential to explain the very high signal seen on this line, and the value of the line ratio $(a\text{-}d)/(k,j)$ is much higher than the high density limit of 1.6 [6,23], because of this phenomenon.

We also give, in Table I, the ratios obtained from experimental spectra when a 10^{16} W/cm^2, ultrashort pulse (400 fs) is incident on a plasma created by a nanosecond prepulse at 10^{10} W/cm^2 [24]. Hydrodynamic simulations of the long, low intensity prepulse interaction indicate a scale length slightly above 1 μm in the neighborhood of the critical surface [26]. The line ratios also indicate such a scale length.

In summary, we have modeled ultrashort pulse laser plasma interaction, and shown that, in a certain range of density scale lengths (0.4–4 μm), both the effects of the rapid time variation and of the non-Maxwellian electron energy distribution functions in the colder regions can be clearly demonstrated by K-shell satellite line ratios, even without any source of energetic electrons, such as resonance absorption (if such a source were present, the effects discussed here would be further enhanced by it). For shorter gradient lengths, the streaming effect is more pronounced, but obscured by collisional mixing and a different diagnostic would need to be devised. In future experiments, these effects may be expected to be even more important. At higher intensity, gradient steepening by the ponderomotive force [27] should enhance the streaming effect, and for higher atomic number (Z) targets, greater thresholds will also tend to increase its importance.

J.P.M. thanks the organizers of the CECAM workshop on short pulse interaction, Professor M. G. Haines and Dr. G. Ciccotti, the other participants, and Dr. J. Virmont and Dr. M. Busquet for useful discussions. We also thank Dr. G. Mourou for his support. This research is supported in part by the Ministère de l'Education du Québec, and by the Natural Sciences and Engineering Council of Canada.

[1] G. Mourou and D. Umstadter, Phys. Fluids B **4**, 2315 (1992).
[2] H. Milchberg *et al.*, Phys. Rev. Lett. **61**, 2364 (1988).
[3] J. C. Kieffer *et al.*, Phys. Rev. Lett. **62**, 760 (1989).
[4] M. M. Murnane *et al.*, Science **251**, 531 (1991).
[5] H. Milchberg, I. Lyubomirsky, and C. G. Durfee III, Phys. Rev. Lett. **67**, 2654 (1991).
[6] A. Zigler *et al.*, Phys. Rev. A **45**, 1569 (1992).
[7] P. Audebert *et al.*, Europhys. Lett. **19**, 189 (1992).
[8] H. Chen *et al.*, Phys. Rev. Lett. **70**, 3431 (1993).
[9] H. R. Griem, Phys. Fluids B **4**, 2346 (1992).
[10] A. H. Gabriel, Mon. Not. R. Astron. Soc. **160**, 99 (1972).
[11] A. R. Bell, R. Evans, and D. J. Nicholas, Phys. Rev. Lett. **46**, 243 (1981).
[12] J. P. Matte and J. Virmont, Phys. Rev. Lett. **49**, 1936 (1982).
[13] G. J. Rickard, A. R. Bell, and E. M. Epperlein, Phys. Rev. Lett. **62**, 2687 (1989).
[14] J. R. Albritton, Phys. Rev. Lett. **50**, 2078 (1983).
[15] J. P. Matte, T. W. Johnston, J. Delettrez, and R. L. McCrory, Phys. Rev. Lett. **53**, 1461 (1984).
[16] J. F. Luciani, P. Mora, and J. Virmont, Phys. Rev. Lett. **51**, 1664 (1983).
[17] E. M. Epperlein and R. W. Short, Phys. Fluids B **3**, 3092 (1991).
[18] M. K. Prasad and D. S. Kershaw, Phys. Fluids B **3**, 3087 (1991).
[19] J. C. Kieffer *et al.*, Phys. Rev. Lett. **68**, 480 (1992).
[20] M. Lamoureux, P. Alaterre, and J. P. Matte, J. Phys. (Paris), Colloq. **47**, C-57 (1986).
[21] A. B. Langdon, Phys. Rev. Lett. **44**, 575 (1980).
[22] O. Peyrusse, Phys. Fluids B **4**, 2007 (1992).
[23] O. Peyrusse *et al.*, J. Phys. B **26**, L511 (1993).
[24] J. C. Kieffer *et al.*, Phys. Fluids B **5**, 2676 (1993).
[25] J. C. Kieffer *et al.*, Proc. SPIE **1860**, 127 (1993).
[26] M. Busquet (private communication).
[27] X. Liu and D. Umstadter, Phys. Rev. Lett. **69**, 1935 (1993).

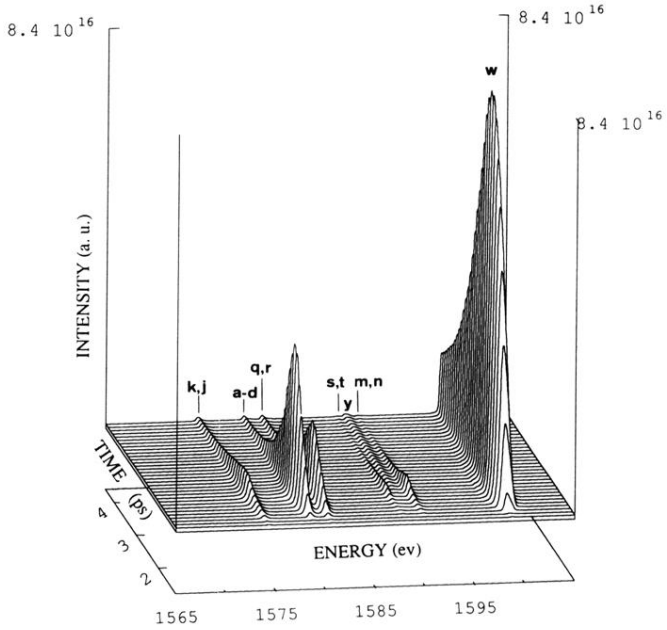

FIG. 1. Synthetic, time-dependent spectrum near the He-α line for the simulation with initial density scale length 1 μm (intensity, 10^6 W/cm^2; 400 fs FWHM; wavelength, 1.06 μm). Lines are labeled following the Gabriel notation [10].